Liquid Crystals
Publication details, including instructions for authors and subscription information:
http://www.informaworld.com/smpp/title~content=t713926090

Synthesis and study of azo dye compounds: variation of mesogenic behaviour with length of alkyl chains

Long-Li Lai Corresponding author[a]; Feng-Ya Su[a]; Chen-Hsiung Hung[b]
[a] Department of Applied Chemistry, National Chi Nan University, Puli, Taiwan 545, ROC [b] Department of Chemistry, National Changhua University of Education, Changhua, Taiwan 500, ROC

To cite this Article Lai Corresponding author, Long-Li , Su, Feng-Ya and Hung, Chen-Hsiung(2004) 'Synthesis and study of azo dye compounds: variation of mesogenic behaviour with length of alkyl chains', Liquid Crystals, 31: 6, 773 — 779
To link to this Article: DOI: 10.1080/02678290310001658390
URL: http://dx.doi.org/10.1080/02678290310001658390

LIQUID CRYSTALS, 2004, VOL. 31, NO. 6, 773–779

Synthesis and study of azo dye compounds: variation of mesogenic behaviour with length of alkyl chains

LONG-LI LAI*, FENG-YA SU
Department of Applied Chemistry, National Chi Nan University, Puli,
Taiwan 545, ROC

and CHEN-HSIUNG HUNG
Department of Chemistry, National Changhua University of Education,
Changhua, Taiwan 500, ROC

(*Received 6 July 2003; in final form 29 October 2003; accepted 2 November 2003*)

The mesogenic behaviours of two azo dye liquid crystals, **1** and **4**, differ because of the different length of terminal alkyl chains; azo dye **1** shows a SmB phase, azo dye **4** shows nematic and SmA phases during thermal processing. The molecular stackings of these two azo dye liquid crystals are compared on the basis of crystallographic studies to explain such unexpected mesogenic behaviour.

1. Introduction

Supramolecular aggregation by molecular self-assembly is an important issue in the filed of structural chemistry [1]. In addition to electrostatic interaction, non-covalent forces also play a significant role in determining the structural stacking and properties of molecular assemblies [2]. The interaction between the functional molecules is found to be critical for molecular packing in crystallization [3], and for the varying mesogenic behaviour of the molecules [4]. Azo dyes **1**–**3** have previously been prepared and their liquid crystalline phases explored in this laboratory. We found that the various conformations of the molecules resulted in various molecular stackings in the solid state; different mesogenic phases were obtained in this way [5]. To expand this study, we have prepared azo dye **4**; unexpectedly, this compound shows nematic and SmA phases during cooling, which is different from the behaviour of azo dye **1**(SmB). Generally, the mesogenic behaviour of liquid crystals may be changed when the rigid cores contain different substituents: a nematic phase may appear when a strong polar group, such as –CN, replaces a non-polar alkyl chains; a smectic phase may appear when the length of a terminal alkyl chain is increased [6]. However, conversion of the SmB phase of azo dye **1** to the nematic and SmA phases of azo dye **4** simply by the variation of alkyl chain length is rather unusual; this has prompted us to study azo dye **4** on the basis of crystallography and to compare in detail the molecular stacking and conformation of azo dyes **1** and **4** in the solid state. Compounds **1** and **4** were further studied by molecular modelling to understand the molecular conformation in the gas phase.

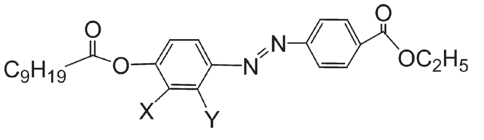

1 X = H, Y=H
2 X = F, Y=H
3 X = H, Y=F

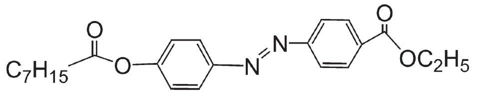

4

Structure.

2. Experimental

Chemicals used were commercially available from ACROS. The mesogenic behaviour and phase transitions were characterized by polarizing optical microscopy (POM) and differential scanning calorimetry (Perkin-Elmer DSC 6). Powder X-ray diffraction (XRD) patterns were obtained from a Siemens D-5000 X-ray diffractometer equipped with a TTK 450 temperature controller and Cu radiation with the wavelength length, $\lambda = 1.5406$ Å. Semi-empirical calculation was carried out by the Cache program using the AM1 model, which was provided by Fujitsu (version 4.1).

---

*Author for correspondence; e-mail: lilai@ncnu.edu.tw.

Liquid Crystals ISSN 0267-8292 print/ISSN 1366-5855 online © 2004 Taylor & Francis Ltd
http://www.tandf.co.uk/journals
DOI: 10.1080/02678290310001658390

2.1. *Synthesis of compound 4*

Compound **4** was prepared in a similar manner to compound **1** according to the scheme and was characterized to be the correct compound by ^{1}H NMR (Varian 300 FT spectrometer), ^{13}C NMR spectra (Bruker 200 FT NMR spectrometer) and high resolution mass spectra (HRMS;VG70-250; EI, 70ev). A solution of phenol (1.88 g, 20 mmol) and KOH (1.12 g, 20 mmol) in H_2O (20 ml) was added to a solution of the diazonium salt **5** (5.17 g, 20 mmol) in ethanol, which was prepared according to a literature method [7]. The solution was then stirred at room temperature for 2 h. The resulting solution was made slightly acidic (pH = 5–6) with aqueous hydrochloric acid. The precipitated product was filtered off and purified by chromatography. Intermediate compound **6** was thus isolated in 45.37% yield (2.45 g). Compound **6** (0.54 g, 2 mmol) was further treated with octanoyl chloride (0.33 g, 2 mmol) in dichloromethane (20 ml) with excess triethylamine to yield crude product **4**, which was further purified by chromatography (Al_2O_3;II). Yield was 0.42g (53.5%) after normal work-up. ^{1}H NMR **4**: δ($CDCl_3$) 0.88 (t, 3H, $J = 6.9$ Hz, CH_3), 1.27–1.43 (m, 11H, $4CH_2 + CH_3$), 1.77 (quint, 2H, CH_2), 2.58 (t, 2H, CH_2), 4.41 (quart, 2H, CH_2), 7.25 (d, 2H, $J = 8.7$ Hz, 2 × Ar–H), 7.92 (d, 2H, $J = 8.7$ Hz, 2 × Ar–H), 7.97 (d, 2H, $J = 8.7$ Hz, 2 × Ar–H), 8.17 (d, 2H, $J = 8.7$ Hz, 2 × Ar–H). ^{13}C NMR: δ($CDCl_3$) 171.83, 165.98 (C = O), 154.97, 153.33, 150.06, 132.20, 130.53, 124.34, 122.57, 122.31, 61.22, 34.40, 31.62, 29.03, 28.88, 24.86, 22.57,14.30, 14.03. HRMS for $C_{23}H_{28}N_2O_4$: 396.2049; found: 396.2052.

2.2. *X-ray crystallography*

Crystals of compound **4** were grown from dichloromethane/hexane (1/1) at room temperature. A single orange crystal of suitable quality was mounted on a glass fibre and used for measurement of precise cell constants and intensity data collection. Diffraction measurements were made on a Siemens SMART CCD diffractometer with graphite–monochromated Mo K_α radiation ($\lambda = 0.71073$ Å), operated at 293(2) K over the θ range of 1.64–25.08°. No significant decay was observed during the data collection. A total of 1 840 reflections were observed with $I \geqslant 2\sigma(I)$ among the 19 602 unique reflections, and 3913 reflections were used in the refinement. Data were processed on a PC using the SHELXTL software package [8]. The structure of **4** was solved using the direct method and refined by full-matrix least square on F^2 value. All non-hydrogen atoms were refined anisotropically. The positions of hydrogen atoms were identified by calculation, and their contributions in structure factors were included. The final indices were $R1 = 0.0940$, $wR2 = 0.2896$ with goodness-of-fit on $F^2 = 1.059$. Other data are as follows: formula $C_{23}H_{28}N_4O_2$; formula weight 396.47; crystal size $0.58 \times 0.50 \times 0.42$ mm^3; unit cell $a = 16.117(4)$, $b = 5.5126(13)$, $c = 49.704(12)$, $\alpha = \gamma = 90°$, $\beta = 93.149(4)°$; crystal system monoclinic; space group *C*2/*c*; volume 4409.3(18) Å^3; cell units (*Z*) 8; density(calcd.) 1.194 g cm^{-3}; linear absorption coefficient 0.082 μcm^{-1}. Coordinates of atoms (C, H, N, O) for compound **4** are listed in table 1.

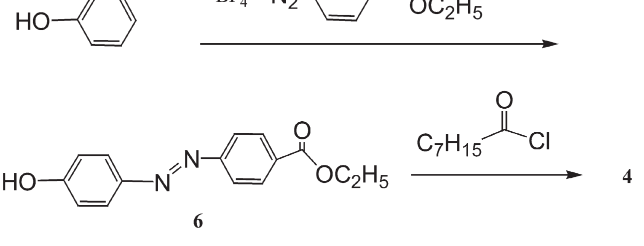

Scheme. Synthesis of azo dye **4**.

Crystallographic data for the compound **4** have been deposited with Cambridge Crystallographic Data Centre as supplementary publication No. CCDC-212023. Copies of the data can be obtained free of charge on application to the Director, CCDC, 12 Union Road, Cambridge CB2 1EZ, UK (fax: +44-1223-336033, e-mail: deposit@ccdc.cam.ac.uk).

3. Results and discussion

3.1. *Synthesis and physical study*

The reaction of phenol with diazonium salt **5** under basic conditions gave compound **6** in about 45% yield; further treatment of compound **6** with octanoyl chloride yielded the desired azo dye **4** in about 53% yield. It was found that azo dye **4** was unstable in acid media but stable during heating in DSC. Azo dye **4** showed nematic and SmA phases during cooling (table 2). The nematic phase was characterized by its schlieren texture together with low viscosity; the SmA phase was characterized by a typical focal-conic texture and low viscosity. To confirm the nematic and SmA phases of compound **4**, it was further studied by powder XRD. As there is no layer structure for liquid crystals in the nematic range, and no reflection at small angle was observed for compound **4** in the range 85.3–78.3°C, the nematic phase of azo dye **4** was further confirmed. Additionally, the *d*-spacing distance (the *z*-component of an extended molecular length) for compound **4** at 75°C was measured as 26.42 Å according to XRD during cooling; the extended molecular length of compound **4** was calculated to be

Table 1. The coordinates (*x y z*) of atoms for compound **4**.

O	0.13539(19)	−0.0577(5)	1.01571(6)
C	0.1518(3)	0.3428(8)	0.94587(9)
N	0.2004(3)	0.4167(8)	0.90680(10)
C	0.2138(3)	0.7942(10)	0.83253(10)
H	0.0571	−0.5026	1.0958
C	0.2029(3)	0.5587(10)	0.88131(11)
H	0.1717	−0.2080	1.0637
C	0.1568(3)	0.7652(12)	0.87594(10)
C	0.0541(3)	−0.5253(9)	1.15079(10)
H	0.0327	−0.6750	1.1429
H	0.0103	−0.1212	1.0806
C	0.2033(3)	0.1507(10)	0.95190(11)
C	0.0861(3)	0.2868(10)	0.98694(11)
C	0.0949(3)	0.4123(10)	0.96361(11)
C	0.1958(3)	0.0246(9)	0.97551(10)
O	0.0734(3)	0.2050(6)	1.04271(7)
H	0.1312	1.0254	0.8473
H	−0.0216	−0.3066	1.1269
C	0.2231(4)	0.9001(13)	0.80583(12)
H	−0.0440	−0.4684	1.1747
C	0.2534(3)	0.4702(12)	0.86266(13)
C	0.2590(3)	0.5845(12)	0.83881(12)
O	0.1769(3)	1.0929(9)	0.80089(8)
C	0.0327(4)	−0.6983(11)	1.19722(12)
H	0.0066	−0.6669	1.2138
C	0.1787(6)	1.2094(16)	0.77459(13)
H	0.2241	1.1423	0.7650
H	0.1215	1.0924	0.7443
H	0.0720	1.0927	0.7706
C	0.1391(3)	0.0962(8)	0.99336(9)
C	0.1029(3)	0.0107(8)	1.03914(9)
N	0.1521(3)	0.4961(8)	0.92112(9)
C	0.0796(3)	−0.3575(7)	1.10449(9)
H	0.1385	−0.3843	1.1085
C	0.1129(3)	−0.1862(8)	1.05920(9)
H	0.0923	−0.3356	1.0510
H	0.1221	0.8252	0.8887
H	0.1137	−0.5441	1.1540
C	0.0690(3)	−0.1461(7)	1.08495(8)
H	0.0907	−0.0001	1.0937
H	0.2433	0.1056	0.9401
H	0.0448	0.3293	0.9984
H	0.0616	0.5471	0.9598
H	0.2293	−0.1097	0.9793
C	0.1622(3)	0.8860(10)	0.85105(10)
C	0.0378(3)	−0.3211(8)	1.13072(9)
H	0.0573	−0.1700	1.1388
C	0.0156(4)	−0.4879(10)	1.17775(10)
H	0.0375	−0.3396	1.1859
H	0.2842	0.3303	0.8663
H	0.2940	0.5216	0.8263
O	0.2675(3)	0.8198(11)	0.78946(10)
H	0.0109	−0.8454	1.1893
H	0.0916	−0.7148	1.2008
H	0.1891	1.3815	0.7771
C	0.1108(6)	1.181(3)	0.76038(19).
H	0.0879	1.3370	0.7556

Table 2. Phase transition temperatures (°C) and corresponding enthalpies ($\mathrm{J\,g^{-1}}$), in parentheses, of compounds **1** and **4**, determined by 2nd DSC scans at a heating and cooling rate of $10^{\circ}\,\mathrm{min}^{-1}$ between 40 and 110°C. Abbreviations: Cr = crystalline, SmX = unidentified smectic phase, N = nematic, SmA = smectic A phase, SmB = smectic B phase, I = isotropic liquid.

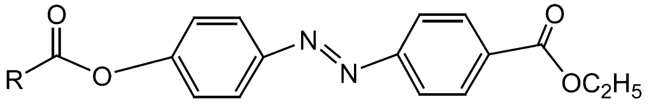

1, $R = C_9H_{19}$ $\quad \mathrm{SmB} \underset{88.4(97.2)}{\overset{95.3(97.9)}{\rightleftharpoons}} \mathrm{I}$

4, $R = C_7H_{13}$ $\quad \mathrm{Cr} \xleftarrow[68.1(56.6)]{} \begin{matrix}\mathrm{Cr}\\ \mathrm{SmA}\end{matrix} \underset{78.3(10.0)}{\overset{83.3}{\rightleftharpoons}} \begin{matrix}\mathrm{SmX}\\ \mathrm{N}\end{matrix} \underset{85.3(1.9)}{\overset{87.3^{a}}{\rightleftharpoons}} \mathrm{I}$

[a] The peak is overlapped and the enthalpy is $84.3\,\mathrm{J\,g^{-1}}$.

25.34 Å by the Cache program on the basis of molecular conformation from the crystallographic data. As liquid crystal molecules in the SmA range are directed along the *z*-axis, the *d*-spacing from the XRD study should be approximately equal to the fully extended length of the molecule; therefore our experimental results are consistent with each other. Although there is difference between the observed *d*-spacing and the calculation data, the variation is insignificant and should be reasonable, as the single crystal structure determination was carried out at 20°C (293 K), and the XRD measurement was made at 75°C.

As indicated previously, the mesogenic behaviour of liquid crystals may change according to the different length of the terminal alkyl chain [6]. However, moving from the SmB phase of azo dye **1** to the nematic and SmA phases of azo dye **4** is rather unusual when only changing the alkyl chain from C_9H_{19} to C_7H_{15}. From previous experience, changed mesogenic behaviour should result from intermolecular interactions between the functional groups of the molecules in the solid state [4, 5, 6 *a*]. Compound **4** was therefore studied by single crystal determination, and its molecular stacking was then established on the basis of the crystallographic data (figure 1). Each molecule of **4** is regularly arranged head-to-head or head-to-tail with adjacent molecules in the same or neighbouring layers. The molecules are found to be parallel to neighbouring molecules in the same layer (e.g. molecules a1 and a2 in the A layer), and the distance between corresponding atoms in the same layers (e.g. Na and Nb, Ca and Cb) are all about 5.51 Å.

The molecules in different layers are also approximately parallel, and the distances between O (CO_2) and aromatic C pairs in adjacent layers (e.g. in A and B layers) are similar: the C5–O5 and C6–O6 distances are both 3.45 Å, and the C1–O1 and C2–O2 distances are both 3.77 Å. Consequently, the distances for H(at C*n*)–O*n* (*n* = 5,6) and H(at C*n*)–O*n* (*n* = 1,2) are very short and calculated to be 2.57 and 2.85 Å, respectively; these distances are shorter than or approximately equal to the sum of the van der Waals radii of H and O atoms (Bondi radii: H 1.20, O 1.52) [9 *a*].

The H-bond interaction between the terminal ethoxycarboxylate moieties of molecules in the same layer seems also significant (e.g. in the B layer). The distances for H (at C*n*)–O*n* (*n* = 3,4) are both 2.75 Å, which are also approximately equal to the sum of the van der Waals radii of H and O atoms. It can be concluded that intermolecular hydrogen bonding contributes significantly to the packing force of compound **4**. It is noteworthy that the aromatic C–H in this case acts as the H-bond donor for the formation of the intermolecular H-bond with an O atom in the liquid crystalline network. This is unusual, but has been observed in other systems [9 *b*–*e*].

Similarly, intermolecular hydrogen bonding contributes significantly to the packing force of compound **1**. On the basis of crystallographic data [5], its molecular stacking has also been established (figure 2). Each molecule of **1** is regularly arranged head-to-head or head-to-tail with adjacent molecules in the same or neighbouring layers. The molecules are also found to be parallel to neighbouring molecules in the same layer (e.g. molecules e1 and e2 in the E layer), and the distances between corresponding atoms in the same layers (e.g. Na and Nb, and Ca and Cb) are all about 5.57 Å. The molecules in different layers are also approximately parallel, and the distances between O (CO_2) and aromatic C in two adjacent layers (e.g. in A and B or E and F layers) are similar: the C5–O5 and C6–O6 distances are both 3.36 Å, and the C1–O1 and C2–O2 distances are both 3.95 Å. Consequently, the distances for H(at C*n*)–O*n* (*n* = 5,6) and H(at C*n*)–O*n* (*n* = 1,2) are calculated to be 2.58 and 3.02 Å, respectively, which are shorter or longer, respectively, than the sum of the van der Waals radii of H and O atoms. Similarly, the H-bond interaction between the terminal ethoxycarboxylate moieties of the molecules in the same layer is also significant (e.g. in the E layer). The distances for H(at C*n*)–O*n* (*n* = 3,4) are both 3.00 Å, which are also the normal length of a H-Bond [9 *b*].

Apparently, the intermolecular H-bonding interactions for H(at C*n*)–O*n* (*n* = 1–4) in compound **1** are different from those in compound **4** (table 3), and this should, to some extent, influence the molecular

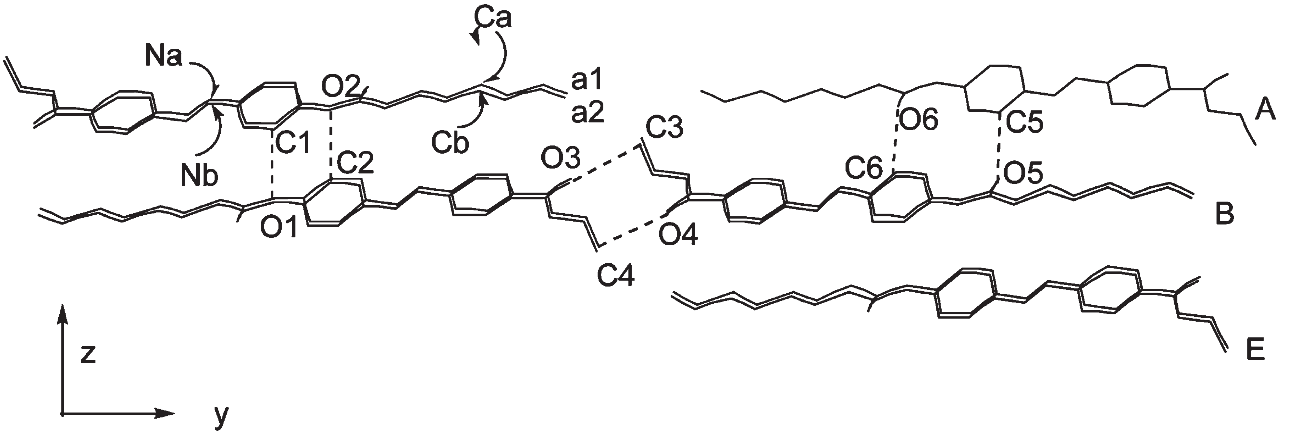

Figure 1. Molecular packing of compound **4** in the solid state. The hydrogen atoms are omitted for clarity.

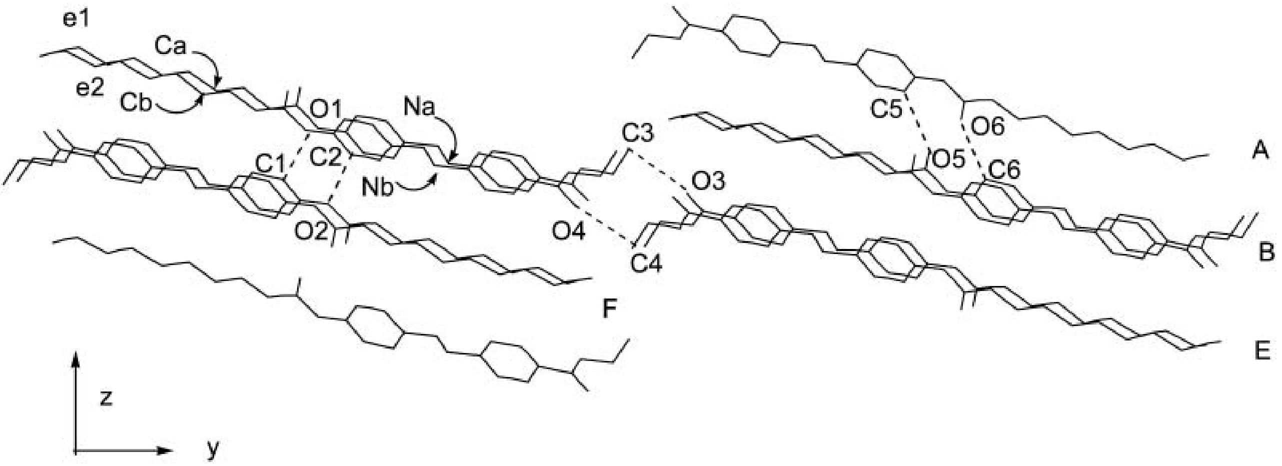

Figure 2. Molecular packing of compound **1** in the solid state. The hydrogen atoms are omitted for clarity.

Table 3. Some intermolecular H-bond distances for compounds **1** and **4**.

Compound	Distances/Å, of H(at C1)–O1 and H(at C2)–O2	Distances/Å, of H(at C3)–O3 and H(at C4)–O4	Distances/Å, of H(at C5)–O5 and H(at C6)–O6
1	3.02	3.00	2.58
4	2.85	2.75	2.57

packing. If the molecular stackings in figures 1 and 2 are viewed along the *z*-direction, then figures 3 and 4 can be obtained. It is interesting to note that the molecules of compound **4** are not in such a highly packed order as those of compound **1**. In the view along the *z*-direction (figure 3), a V-shaped arrangement can be observed. As indicated in the previous study, various conformations of the molecules can result in various molecular stackings in the crystallization process [4, 5]. It seems reasonable to suggest that the

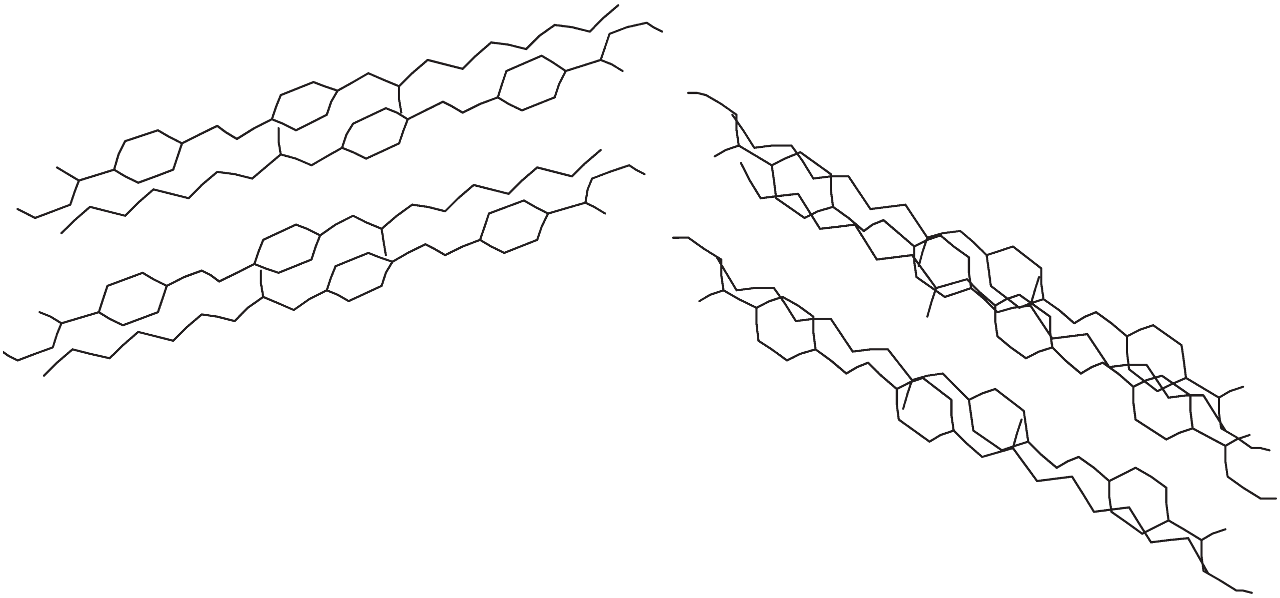

Figure 3. Molecular packing of compound **4** in the solid state: view along the *z*-direction. The hydrogen atoms are omitted for clarity.

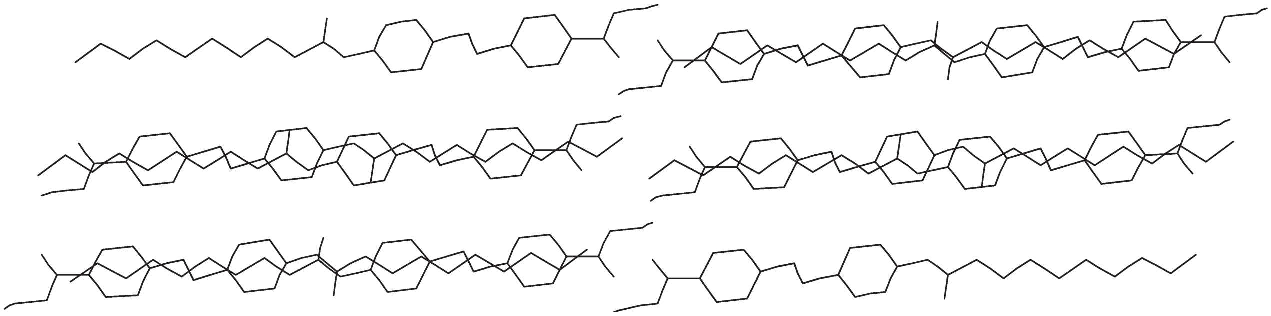

Figure 4. Molecular packing of compound **1** in the solid state: view along of *z*-direction. The hydrogen atoms are omitted for clarity.

various molecular stackings for compounds **1** and **4** (figures 1–4) may have the same origin.

To understand the influence of these H-bondings on the conformation of the azo dye molecules in the solid state, the bond distances Oa–Cy and Ha′–Ob′, together with the dihedral angles Oa–Cx–Ob–Cy and Ha′–Cx′–Cy′–Ob′ for compounds **1** and **4** have been calculated (table 4 and figure 5), as a different extent of intermolecular H-bond interaction arises in the corresponding moieties of the molecules. It is noteworthy that the dihedral angles Ha′–Cx′–Cy′–Ob′ in compounds **1** and **4** are calculated to be 0.25° and 3.32°, respectively, on the basis of the crystallographic data. Apparently, the stronger interaction of intermolecular H-bonding in the corresponding moieties of compound **4** makes its conformation to some extended twisted and bent in the solid state; the solid stacking of compound **4** is therefore different from that of compound **1** during crystallization. It is known that an SmA phase liquid crystal possesses a layer structure. Additionally, if a

Table 4. Some distances of atom pairs and dihedral angles for compounds **1** and **4**.

Compound	Distance of Oa–Cy/Å	Dihedral angle of Oa–Cx–Ob–Cy/°	Distance of Ha'–Ob'/Å	Dihedral angle of Ha′–Cx′–Cy′–Ob′/°
1	2.68	1.05	2.42	0.25
(optimized)[a]	(2.63)	(0.48)	(2.57)	(4.69)
4	2.69	1.15	2.38	3.32
(optimized)[a]	(2.63)	(0.49)	(2.57)	(4.87)

[a] The optimization was completed on the basis of the original conformation from crystallographic data.

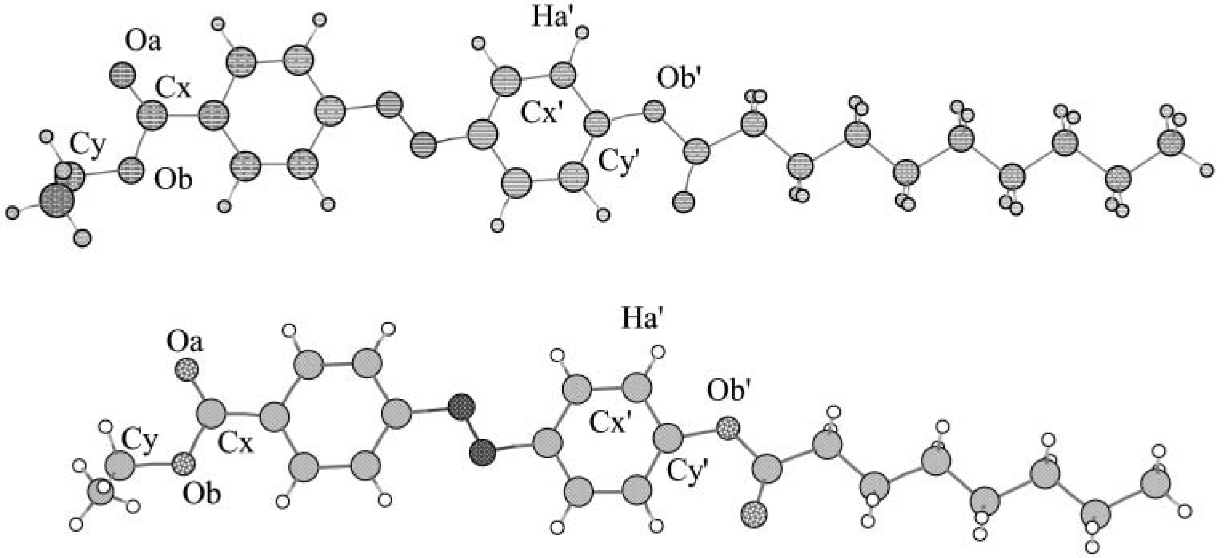

Figure 5. The conformation of a single molecule for compounds **1** and **4**.

regular hexagonal arrangement exists within the SmA layer structure, a SmB phase can be obtained. From the crystallographic study, an intermolecular bending has been observed in the network of compound **4**. This bending should distort the molecular stacking and result in breaking the regular hexagonal arrangement seen in compound **1**, while maintaining the layer structure. This leads to the observation of SmA and nematic phases in compound **4** during DSC.

The conformations of azo dyes **1** and **4** were further optimized by the CaChe program, using the AM1 model in the gas phases. After optimization, the Oa–Cy and Ha′–Ob′ bond distances together with the dihedral angles Oa–Cx–Ob–Cy and Ha′–Cx′–Cy′–Ob′ for compounds **1** and **4** were further calculated (table 4 and figure 5). The corresponding bond distances and dihedral angles are not significantly different from each other. This indicates that in the gas phase, the conformations of molecules **1** and **4** are not significantly different from each other because of the absence of intermolecular

H-bonding. However, in the solid state, the conformations of molecules **1** and **4** are affected by H-bond interaction between molecules, and different molecular stackings and mesogenic behaviour are thus obtained.

4. Summary

We have shown how two azo dyes, **1** and **4**, having the same rigid core and different length of terminal alkyl chain, possess different mesogenic behaviour, on the basis of crystallographic study together with the calculation of intermolecular H-bond distances. The stronger the H-bond interaction of the molecules, the more bent or twisted the conformation of molecules obtained in the solid state. Using this approach, we demonstrate that the H-bond interaction between molecules plays an important role in molecular stacking in the solid state, and consequently, results in varied mesogenic behaviour of the azo dye liquid crystals.

We thank the National Chi Nan University and the National Science Council (NSC 91-2113-M-260-006) for financial support. The National Center for High-Performing Computing and the Institute of Chemistry, Academia Sinica are also highly appreciated for providing, respectively, the Beilstein database system, and a most helpful library service.

References

[1] (*a*) LEHN, J.-M., 1995, *Supramolecular Chemistry* (Weinheim: VCH); (*b*) HAMILTON, A. D., 1996, *Perpectives in Supramolecular Chemistry* (New York: John Wiley).

[2] (*a*) HUNTER, C. A., 1993, *Angew. Chem. int. Ed. Engl.*, **32,** 1584; (*b*) HUNTER, C. A., 1994, *Chem. Soc. Rev.*, **23,** 101.

[3] (*a*) DESIRAJU, G. R., 1989, *Crystal Engineerring: The Design of Organic Solids* (New York: Elsevier); (*b*) DESIRAJU, G. R., 1997, *Chem. Commun.*, 1475.

[4] (*a*) LEE, K. M., LEE, C. M., and LIN, I. J. B., 1997, *Angew. Chem. int. Ed. Engl.*, **36,** 1850; (*b*) CHANG, J., and MOORE, J. S., 1994, *J. Am. chem. Soc.*, **116,** 2655.

[5] LAI, L. L., SU, F. Y., LIN, Y. J., HO, C. H., WANG, E., HUNG, C. H., LIU, Y. H., and WANG, Y., 2002, *Helv. Chim. Acta*, **85,** 1517.

[6] (*a*) LAI, L. L., HO, C. H., LIN, Y. J., WANG, E., LIU, Y. H., WANG, Y., LIN, Y. C., and CHENG, K. L., 2002, *Liq. Cryst.*, **29,** 1477; (*c*) PETROV, V. F., 2001, *Liq. Cryst.*, **28,** 217.

[7] LAI, L. L., and LIN, H.-C., 2000, *Liq. Cryst.*, **27,** 707.

[8] SHELDRICK, G. M., 1994, *SHELXTL*, version 5.03, Siemens Analytical X-ray Instruments Inc. (Madison, WI: Siemens).

[9] (*a*) BONDI, A., 1964, *J. phys. Chem.*, **68,** 441; (*b*) ALLEN, F. H., LOMMERSE, J. M. P., HOY, V. J., HOWARD, J. K. H., and DESIRAJU, G. R., 1996, *Acta Cryst.*, **B52,** 734; (*c*) THAIMATTAM, R., XUE, F., SARMA, J. A. R. P., MAK, T. C. W., and DESIRAJU, G. R., 2001, *J. Amer. chem. Soc.*, **123,** 4432; (*d*) MUTHURAMAN, M., MASSE, R., NICOUD, J.-F., and DESIRAJU, G. R., 2001, *Chem. Mater.*, **13,** 1473; (*e*) CIUNIK, Z., and DESIRAJU, G. R., 2001, *Chem. Commun.*, 703.